Proceedings of the International Conference on Heat Exchanger Fouling and Cleaning - 2024 (Peer-reviewed)
April 21–26, 2024, Lisbon, Portugal; Editors: H.U. Zettler and E.M. Ishiyama

Prognostics of heat exchanger fouling via inference with symbolic regression

Efi Safikou[1] and George Bollas[2,*]
[1] Department of Electrical & Computer Engineering, University of Connecticut, Storrs, CT 06269, USA
email: efstathia.safikou@uconn.edu
[2] Department of Chemical & Biomolecular Engineering, University of Connecticut, Storrs, CT, 06269, USA
email: george.bollas@uconn.edu

ABSTRACT

Fault diagnostics and prognostics serve as invaluable tools for effective system health management and monitoring. We first develop inferential sensors, which are sensitive to fouling and remain unaffected by uncertainty, through symbolic regression combined with information theory. Adopting these sensors as health indicators, we build a real-time fault prognostic scheme for estimating the progression of fouling in a plate-fin heat exchanger system and estimate its remaining useful life. This technique fuses modeling methods and regression-based approaches to conduct parameter trending. Here, symbolic regression is employed for parameter trending, by utilizing a genetic programming algorithm. This algorithm integrates the system model based on the inferential sensor data and identifies the temporal occurrence of faults (i.e., fouling). The outcome is an estimated function of fouling as a time relationship that analytically describes its future progression. To validate our approach, we apply a dynamic degradation regression model that includes the same health indicators. Both methods are tested over operation of the studied system at various levels of measurement noise and uncertainty. We proved that the proposed hybrid predictive approach provides more accurate predictions for fault occurrence and the remaining useful life of the system compared to a degradation model.

NOMENCLATURE

Acronyms

AI	Artificial Intelligence
ML	Machine Learning
SVM	Support Vector Machines
GP	Genetic Programming
RUL	Remaining Useful Life
PFHE	Plate-fin Heat Exchanger

Symbols

f	Set of governing equations
h	Set of output mapping equations
$\mathbf{x}$	State variables
$\mathbf{u}$	Admissible system inputs
$\boldsymbol{\theta}$	Model parameters
$\boldsymbol{\xi}$	Fault and uncertainty parameters
t	Time
$\hat{\mathbf{y}}$	System output measurements
$\tilde{\boldsymbol{y}}$	Estimated system outputs
z	Inferential sensor function
$\hat{z}$	Inferential sensor measurements
$\tilde{z}$	Estimated inferential sensor
M	Parameter of the degradation model
$\boldsymbol{B}$	Parameter of the degradation model
q	Generated function in GP
N	Number of timesteps included in the time window
$\dot{m}_{h,i}$	Hot air – Mass flow rate
T_c	Cold outlet temperature
T_h	Hot outlet temperature
R_f	Thermal fouling resistance in the cold stream side
ω_{H2O}	Moisture Content
T_{in}^{cold}	Cold air inlet temperature

Subscripts

j	Timestep index in the expanding window for the hybrid method
i	Timestep index in the sliding window for the degradation model method
f	Faults
p	Design and model
q	System uncertainty

Superscripts

$*$	Optimal solution

INTRODUCTION

Diagnostics and prognostics are crucial fields for cyber-physical systems, as they facilitate efficient system monitoring that ensures safety [1]. Diagnostics involve the identification and isolation of faults by leveraging prior knowledge of the entire system operation. Prognostics, on the other hand, offer forecasts of future system conditions and potential failure timelines based solely on present or historical information [2]. Preventing system faults and failures can result in substantial cost savings; therefore, extensive research has been dedicated in developing methods for system fault prognosis [3]-[9].

The most traditional prognostic methods are the so-called physics-based approaches, where we take into consideration the physical knowledge of the

ISBN: 978-0-9984188-3-4; Published online www.heatexchanger-fouling.com

system of interest [10]-[11]. These approaches can be very accurate, as uncertainties in models arising from intangible physical phenomena and/or complex system features are significantly reduced. However, the implementation of such tools can be challenging and computationally demanding. This is often due to the need for a substantial number of experiments, which comes with a high computational load and time requirement [12].

Over the last few years, data-driven approaches have been developed and applied toward providing forecasts, because of the rapid advancement of Artificial Intelligence (AI) [13]. Advanced machine learning (ML) techniques for classification and regression, such as Support and Relevance Vector Machines (SVM) [19]-[25], are widely utilized in the domains of diagnostics and prognostics. These methods, which build models based directly on current and historical data without requiring any physical system knowledge, often yield satisfactory results [14]-[18]. Consequently, they substantially decrease the computational load associated with physics-based approaches [12].

Another set of effective prognostic methods includes specific deep learning techniques, such as auto-encoders, artificial, recurrent, and convolutional neural networks. These methods are extensively employed in health management and prognostics modeling because of their capability to handle more complex data structures, as noted in [26]-[28].

However, the lack of physical system knowledge in both aforementioned methods may lead to substantial modelling inconsistencies that entail systematic errors to the fault estimates. Consequently, the fault identification is becoming more challenging.

Finally, hybrid approaches, founded on the fusion of physics-based and data-driven methods, have arisen to create comprehensive frameworks [29]-[31]. These approaches have gained increasing attention recently, as they leverage the benefits of both concepts and effectively address their limitations [32].

In this work, we attempt to conduct fault prognosis by developing an advanced hybrid method coupled with inferential sensors. More specifically, we combine system modeling methods and regression-based approaches. Symbolic regression is used through a genetic programming algorithm that generates time relationships (i.e., individuals) of the fouling progression of a plate-fin heat exchanger system, given inferential sensor data. Each individual is introduced into the model to estimate the system outputs, as well as the inferential sensor values, and is evaluated by considering the mean squared error of the measured data. The obtained function offers an analytical representation of the evolution of system faults over time. In this regard, we can estimate potential failure initiation instances, as well as the remaining useful life (RUL) of the system. Ultimately, the proposed method is compared with a traditional predictive tool, namely a degradation regression model. The foregoing model is applied to the inferential sensor data within a pre-defined time window to anticipate its future trajectory. It is worth noting that the employed inferential sensors are functions of system outputs and are also derived through genetic programming, which incorporates a combination of symbolic regression and information theory; see also [33]. The latter enhances the sensitivity to faults, while intentionally neglecting evidence of uncertainty. It is important to note that this work does not include a real-life plate-fin heat exchanger. Consequently, no real-life validation or empirical testing has been conducted or presented within this study. The background and the source of the output data used in this work are derived from a heat exchanger system model, which is described in the next section.

METHODOLOGY

The studied system and proposed methods are presented in detail in the following paragraphs.

Heat Exchanger System Model

In this work, a plate-fin heat exchanger system is studied, which consists of a set of differential-algebraic equations that essentially cover all the physical knowledge of the nonlinear system [33, 36]:

$$\mathbf{f}(\dot{\mathbf{x}}(t), \mathbf{x}(t), \mathbf{u}(t), \boldsymbol{\theta}, t) = 0 \qquad (1)$$

where, $\mathbf{f}$ represents the governing equations of the system, $\mathbf{x}(t)$ is the vector of state variables, $\dot{\mathbf{x}}(t)$ denotes the time derivatives of $\mathbf{x}$, $\mathbf{u}(t)$ signifies the admissible inputs, $\boldsymbol{\theta}$ the model parameters, and t denotes the time. The inputs of the system, $\mathbf{u}(t)$, include the controllable system inputs, $\mathbf{u}_p(t)$, and the uncertain inputs, $\mathbf{u}_q(t)$, while the measured outputs (also called hard sensors) of the system, $\hat{\mathbf{y}}$, are given by:

$$\hat{\mathbf{y}} = \mathbf{h}(\mathbf{x}(t), \mathbf{u}(t), \boldsymbol{\theta}, t) \qquad (2)$$

The vector $\boldsymbol{\theta}$ includes the model parameters that represent (i) the faults, $\boldsymbol{\theta}_f$, (ii) the system uncertainty, $\boldsymbol{\theta}_q$, as well as (iii) the system design, $\boldsymbol{\theta}_p$. Note that in a fault detection problem, the parameters of interest typically include faults, uncertain parameters, and uncertain inputs. In this context, we consolidate these parameters into a new vector, $\boldsymbol{\xi}$, and categorize them into the subset declaring faults, denoted as $\boldsymbol{\xi}_f$, and the subset representing uncertainty, denoted as $\boldsymbol{\xi}_q$: $\boldsymbol{\xi} = [\boldsymbol{\theta}_f, \boldsymbol{\theta}_q] \cup [\mathbf{u}_q] = [\boldsymbol{\xi}_f, \boldsymbol{\xi}_q]$.

Inferential sensing

Inferential sensors collect information from other available variables or parameters of the system to estimate a parameter of interest. In our previous work [33], these sensors were specifically designed

ISBN: 978-0-9984188-3-4; Published online www.heatexchanger-fouling.com

to be highly responsive to faults while disregarding the impact of uncertainty. Thereby, they provide enhanced fault detection capabilities.

An inferential sensor, $\hat{z}$, is derived through a Genetic Programming (GP) algorithm using symbolic regression. The objective function of this optimization algorithm was the D_s-optimality criterion for the hard sensors along with a symbolically regressed equation (i.e., the inferential sensor). Note that this equation is a function of the hard sensors. For more comprehensive information, readers are encouraged to refer to [33]. In this study, the obtained inferential sensor is utilized as a health indicator for the following prognostic methods.

Hybrid Prognostic Method

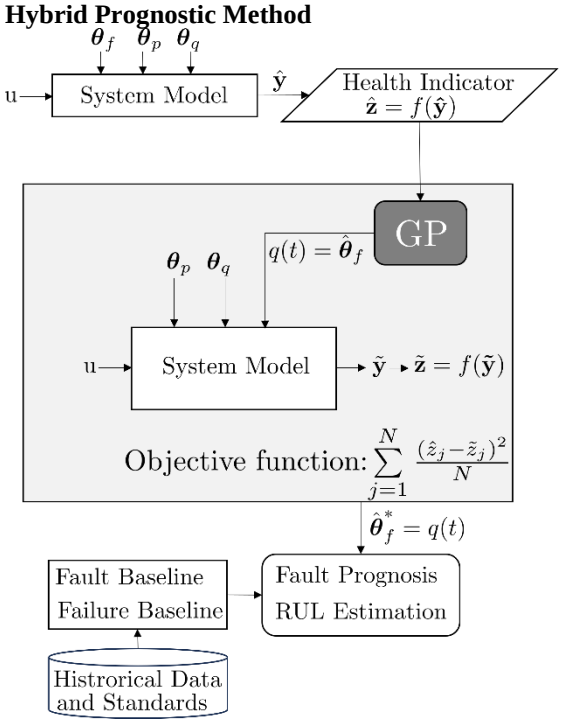

Fig. 1. Flow chart of the proposed hybrid prognostic method.

Figure 1 shows a flowchart of the proposed hybrid prognostic approach. The main goal is the prediction of a potential fault instance and the estimation of system's remaining useful life (RUL).

The prediction of system performance considers both past and current data of the inferential sensor (i.e., $\hat{z}$), which correspond to the measurements of the N timesteps from the initial time until the current time. These data are introduced to a Genetic Programming (GP) algorithm, which generates symbolic regression models. The latter are time relationships q(t), that depict the functions of the estimated fault parameter of the heat exchanger (i.e., fouling). Every generated function is inserted into the system model to estimate the hard sensor data (i.e., $\tilde{y}$) and finally the inferential sensor data (i.e., $\tilde{z}$). For model assessment, we consider the mean square error of the measured inferential sensor; see the objective function in Fig. 1.

The outcome of the GP process is an optimal fouling function, which completes the model and provides the most accurate predictions of the available data. Finally, this estimated fault function is utilized to estimate possible fault instances and system's RUL. Then, we identify the points where the trended fault function intersects the predefined fault threshold (i.e., the fault initiation) and failure timeline (i.e., end of system life). The former is denoted as the predicted fault detection time, while the latter as failure time instance. Finally, the RUL can be estimated by subtracting the current time step from the forecasted failure instance.

Degradation Regression Model

Over time, many research endeavors have utilized degradation regression models, including linear, exponential, or power forms. These models aim to depict future trends in various health indicators and predict the RUL of a system [34]-[35].

We consistently employ a dynamic degradation regression model, which is calibrated with the health indicator (i.e., here, inferential sensor) data of the evolving degradation trend. As time advances, the degradation model is adapted and refreshed using a sliding or expanding window that encompasses both current and historical data of the inferential sensor. Then, we leverage this model to forecast its future trajectory. In this context, predicting potential fault occurrences and the RUL is simplified. Detection of impending faults occurs when the predictive path of the inferential sensor reaches a predetermined fault baseline, while determining RUL involves counting the number of time steps from current time until an anticipated failure threshold is reached.

In this study, the degradation regression model is considered a power function $z = Mt^B$. The values for the parameters M and B are calculated by fitting the degradation model across the sliding window. This is achieved by solving the below optimization problem:

$$\arg\min_{M,B}\{\sum_{i=1}^{N}(z_i - Mt_i{}^B)^2 + \sum_{i=1}^{N}(\dot{z}_\iota - MBt_i{}^{B-1})^2\} \quad (3)$$

where, N is the number of timesteps included in the sliding window, z_i is the value of the inferential sensor, while $\dot{z}_\iota$ represents its slope at time t_i within the sliding window. Notably, the minimization of slope is crucial for capturing additional information from the degradation trajectory, thereby enhancing the precision of the estimations.

CASE STUDY DESCRIPTION

As it is already mentioned, the proposed methods are applied to a crossflow plate-fin heat exchanger (PFHE) system [36]. The input of the system is the mass flow rate of the hot stream, $u = \dot{m}_{h,i}$ (in kg/sec), and the system output measurements are the cold and hot outlet

ISBN: 978-0-9984188-3-4; Published online www.heatexchanger-fouling.com

temperatures, $y = [T_c, T_h]$ (in °C). The inferential sensor which serves as health indicator is given by the equation below:

$$z = (-190.802T_c + 178.716T_h - 2T_c(-T_c + T_h + 6.575) + 1139.9)/(-1488.7) \quad (4)$$

The fault studied in the heat exchanger system is the thermal fouling resistance in the cold stream side, $\theta_f = R_f$ (in $\times 10^{-3}$m^{2}K/W), while the system uncertainty can be found in the cold air inlet stream moisture content, ω_{H2O} (in kg H_2O/kg dry air), and the cold air inlet temperature, T_{in}^{cold} (in °C).

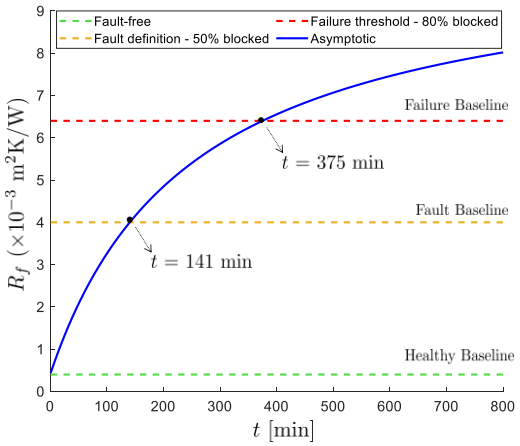

Fig. 2. The injected asymptotic form of the crossflow plate-fin heat exchanger (PFHE) fouling.

Here, we assume that the fault increases asymptotically with time, as shown in Fig. 2. The asymptotic function integrated into the PFHE model is given by $R_f = \frac{10\,t}{t+250} + 0.4$. In the figure, we can see that at the beginning the system is in fault-free condition (i.e., $R_f = 0.4$), and afterwards the fault level rises until the system reaches the failure conditions (i.e., 100% blocked fouling, $R_f = 8$).

It is considered that the 50% blocked state (i.e., $R_f = 0.4$) serves as a threshold requiring the detection of system faults, whereas the 80% blocked state (i.e., $R_f = 8$) marks the end of the system's lifespan. Particularly, in Fig. 2, it can be noted that the fault occurs at t = 141 min, while the termination of the system's lifespan happens at t = 375 min. The responses of the hard (i.e., system outputs) and the inferential (i.e., z) sensors are illustrated in Fig. 3, for different uncertainty levels in moisture content, ω_{H2O} (in kg H_2O/kg dry air), and in the cold air inlet temperature, T_{in}^{cold} (in °C). As shown, z is less affected by changes in uncertainty.

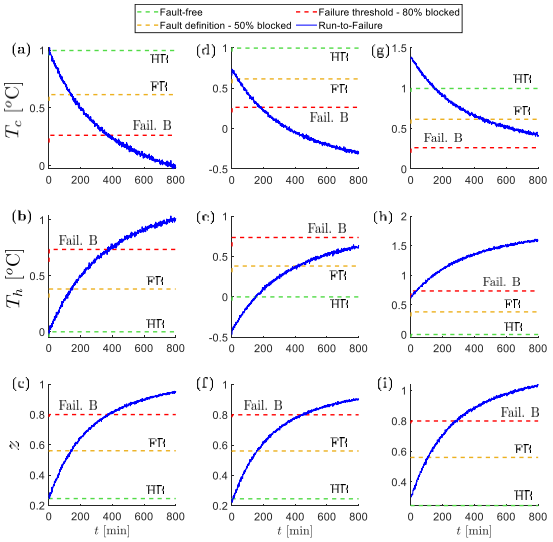

Fig. 3. The hard and inferential sensor responses for three different uncertain scenarios with values: (a-c) $[\omega_{H2O}, T_{in}^{cold}] = [6,45]$, (d-f) $[\omega_{H2O}, T_{in}^{cold}] = [5.3,39]$, and (g-i) $[\omega_{H2O}, T_{in}^{cold}] = [7.3,54]$.

It is important to mention that prognostics are conducted based on the scenario shown in Figs. 3.a-c, which includes the mean values of the uncertain parameters; see also [33].

METHOD IMPLEMENTATION

Hybrid Prognostic Method

The proposed hybrid prognostic method relies on all available present and past data and provides the best estimated relationship of fault with time. Moving in time, new inferential sensor values are incorporated, while simultaneously retaining all past instances of the time series. In this context, the sliding window is consistently expanding.

To evaluate the method, we conduct prognostics at intervals of 50 min with a sampling rate of 1 minute, starting from the initiation of the simulation and continuing until the end of the system's lifespan. In each iteration, a trended fault function is obtained and used to estimate the RUL.

In Table 1, we can see the estimates for potential fault instances and the RUL, as well as their actual values. Additionally, it provides developed analytical expressions illustrating the evolution of system fouling over time. Note that in the initial two iterations, when the system is still free of faults, predictions for fault occurrence are also presented. As indicated, in the first 50 min the method incorrectly forecasts the fault occurrence within 175 min, compared to the real value of 91 min. As far as the RUL, the estimated fouling function never meets the failure threshold, resulting in an infinite RUL value. This implies that, based on the current system condition where faults are absent or at insignificant levels, the method foresees no future failure. Consequently, due to limited system information (specifically in the case of the first

ISBN: 978-0-9984188-3-4; Published online www.heatexchanger-fouling.com

iteration), the symbolic regression scheme fails to capture the behavior of the fault. This leads to a substantial gap between the estimates and the actual values.

In the second iteration, these discrepancies significantly diminish, resulting in a very close estimation for the fault instance with only a 2 min deviation from the actual value and a 9 min error RUL prediction. Although the numerical results are satisfactory, it is important to note that the quantity of data remains insufficient for the development of a precise analytical fault function.

Table 1. Predictions for potential fault instances and the RUL based on the hybrid method, accompanied by the derived fault functions for each iteration.

	Fault Prognosis $[min]$:		RUL $[min]$:		
Current Time $[min]$	Estimated	Real	Estimated	Real	$\hat{R}_f$ $[\times 10^{-3} m^2 K/W]$
50	175	91	∞	325	$\frac{5.06t}{t+91.19} + 0.4$
100	39	41	266	275	$\frac{10t}{t+243.9} + 0.4$
150	-	-	217	225	$\frac{10t}{t+244.66} + 0.4$
200	-	-	173	175	$\frac{10.10t}{t+254.5} + 0.4$
250	-	-	125	125	$\frac{10t}{t+249.66} + 0.4$
300	-	-	75	75	$\frac{10.05t}{t+251.01} + 0.4$
350	-	-	25	25	$\frac{10*t}{t+250.5} + 0.4$

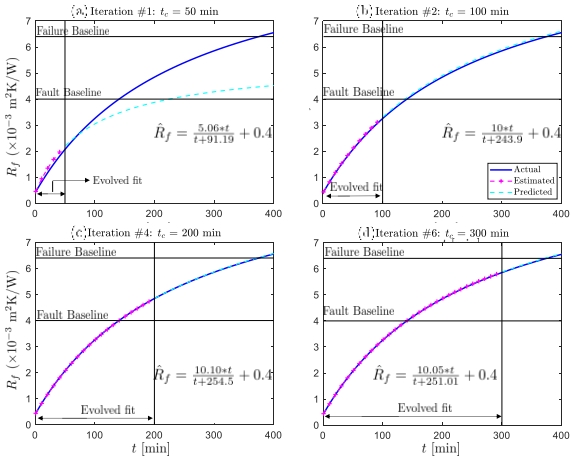

Fig. 4. The estimated fault progression compared with the actual fault trend at time instances: (a) 50, (b) 100, (c) 200 and (d) 300 min.

Figure **Error! Reference source not found.** illustrates the anticipated growth of the estimated fault (represented by the cyan dashed line), compared with the actual increase (depicted by the blue solid line) at time instances of 50, 100, 200 and 300 min. As depicted, the trajectory of the estimated fault in the first iteration (see Fig. 4.(a)) diverges notably from the actual fault function. Conversely, in the second iteration, the estimated fault increase aligns more closely with the actual trend (see Fig. 4.(b)).

As previously stated, our objective is to predict the RUL with high precision. In both time instances, at 200 and 300 min (see Figs 4.(c) and 4.(d)), the trended fault functions almost align with the actual increase, signifying highly accurate RUL values. This is also confirmed by the results in Table 1, where the analytical expressions of $\hat{R}_f$ closely resemble the actual fault function, R_f. Specifically, at $t_c = 200$ min, the RUL estimation is 173 min, differing only 2 min from the real value (i.e., 175 min), while at $t_c = 250$ min the method gives an accurate RUL prediction with zero error. The findings above highlight that the accuracy of the estimates improves over time.

Degradation Regression Model

The degradation regression model introduced in this study relies on a sliding window of 50 min (or the last 50 historical time instances, given a sampling rate of 1 min) for the purpose of forecasting fault occurrences and estimating the RUL. As the sliding window of inferential sensor values moves forward one step, incorporating a new value, the oldest time instance is removed. This chosen degradation regression model is iteratively applied to each updated window, predicting the future track of the inferential sensor until the failure threshold is met.

Table 2 provides the optimal values of the tuned parameters M and B in each iteration, as well as the fault time instances and RUL estimations along with their actual values. In the first iteration, the scheme fails to predict accurately both the time of the fault and the RUL.

Table 2. Predictions for potential fault instances and the RUL based on the degradation model, accompanied by the derived fault functions for each iteration.

	Fault Prognosis $[min]$:		RUL $[min]$:		
Current Time $[min]$	Estimated	Real	Estimated	Real	$\hat{z} = M * t^B$
50	162	91	1410	325	$0.1589t^{0.2203}$
100	38	41	231	275	$0.0743t^{0.4096}$
150	-	-	202	225	$0.0789t^{0.3952}$
200	-	-	148	175	$0.0799t^{0.3939}$
250	-	-	108	125	$0.0892t^{0.3731}$
300	-	-	72	75	$0.1081t^{0.3382}$
350	-	-	28	25	$0.1325t^{0.3029}$

From the next iteration onward, however, the predictions appear noticeably enhanced. At $t_c = 100$ min, the forecast for the fault occurrence is 38 min, which is only 3 min earlier than the actual fault occurrence. However, in terms of the RUL estimation, there is still a considerable deviation from the real value, resulting in an error of 44 min. Then, at $t_c = 200$ min, the method provides 148 min for RUL, which closely approximates the actual value, while at $t_c = 300$ min the method prognose 72 min RUL with an error of 3 min.

ISBN: 978-0-9984188-3-4; Published online www.heatexchanger-fouling.com

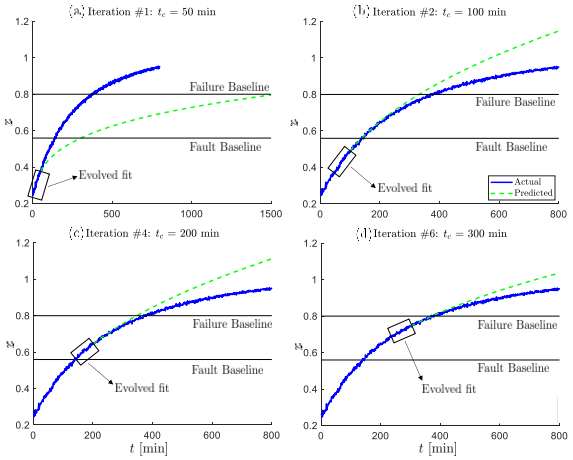

Fig. 5. The degradation regression model of z compared with its actual future values at time instances: (a) 50, (b) 100, (c) 200 and (d) 300 min. Note that, the sliding window used for fitting includes 50 timesteps.

Figure 5 illustrates the available inferential sensor data employed in the fitting process within the sliding window, along with its projected future values represented by dashed lines. As mentioned earlier, the fault occurrence is identified when the future trend reaches the pre-defined fault threshold, while the end of the system's life is predicted when the trend intersects the failure threshold.

In the first iteration (see Fig. 5.(a)), the method does not forecast any fault occurrence in the near future, while the estimated value for RUL significantly differs from the true value. At time $t_c = 100$ min (see Fig. 5.(b)), however, the predictive trend of the inferential sensor more closely aligns with the actual values. As time progresses, it becomes evident that these deviations decrease significantly, as illustrated in Figs 5.(c) and 5.(d).

Comparisons

A comparison between the two approaches is demonstrated in Fig. 6. Specifically, Fig. 6.(a) provides the RUL estimations yielded by both schemes. In the initial iteration, both estimates approach infinity and have been excluded from the graph. In subsequent iterations, it becomes evident that the estimates from both methods progressively converge towards the actual values, with the hybrid method providing more accurate predictions than the degradation model. The full convergence for the hybrid method comes in the last three iterations, while the degradation model provides accurate predictions in the last two iterations.

The differences among the proposed strategies become apparent in Fig. 6.(b), where the absolute variances between the predicted and actual values are illustrated. Clearly, as time advances, the performance of both methods in estimating the RUL shows significant enhancement. Notably, errors markedly decrease after the second iteration (i.e., at 100 min), while they become negligible in the last two iterations, 300 min into the process. It's noteworthy that the discrepancies between the prognostic forecasts and the real RUL values are notably smaller for the hybrid approach, providing evidence of the scheme's heightened robustness.

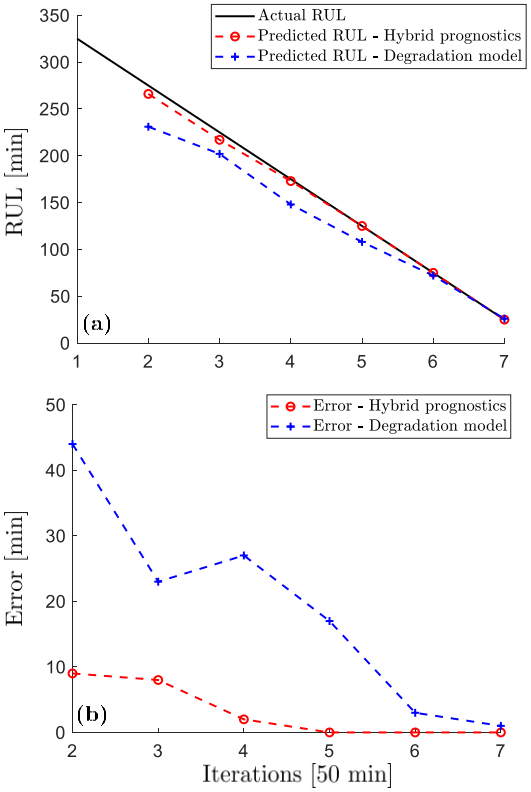

Fig. 6. (a) The RUL values estimated in every 50 min by both methods compared with the true values in each iteration. (b) The absolute errors between the estimated and actual RUL values for both methods in every iteration.

CONCLUSIONS

In this work, a hybrid prognostic technique, fusing system modeling and symbolic regression methods, was proposed. For method assessment, this method was compared to another traditional predictive scheme, which relies on the degradation regression model. Both methods integrated as health indicator an optimized inferential sensor that is designed to be sensitive to faults and unaffected by system uncertainty, through a unique combination of symbolic regression and information theory. By applying both methods in a crossflow plate-fin heat exchanger (PFHE), we showed that the proposed hybrid predictive approach provided more accurate predictions for fault occurrence and RUL compared to a degradation model. This robust performance was complemented by the inclusion of an analytical expression, detailing the evolution of system faults over time.

ISBN: 978-0-9984188-3-4; Published online www.heatexchanger-fouling.com

REFERENCES

[1] Vogl, G.W., Weiss, B.A., and Helu, M., A review of diagnostic and prognostic capabilities and best practices for manufacturing, J Intell Manuf, vol. 30, pp. 79-95, 2019, 10.1007/s10845-016-1228-8.

[2] Biggio, L., and Kastanis, I. (2020) Prognostics and Health Management of Industrial Assets: Current Progress and Road Ahead, Front Artif Intell, vol. 3, 10.3389/frai.2020.578613.

[3] Palmer K. A. and Bollas G. M., "Active fault diagnosis for uncertain systems using optimal test designs and detection through classification," ISA Transactions, vol. 93, pp. 354–369, 2019.

[4] Hale W. T. and Bollas G. M., "Design of Built-In Tests for Active Fault Detection and isolation of Discrete Faults," IEEE Access, vol. 6, pp. 50 959–50 973, 2018.

[5] Awasthi U., Palmer K. A., and Bollas G. M., "Optimal test and sensor selection for active fault diagnosis using integer programming," Journal of Process Control, vol. 92, pp. 202–211, aug 2020.

[6] Biggio L. and Kastanis I., "Prognostics and Health Management of Industrial Assets: Current Progress and Road Ahead," Frontiers in Artificial Intelligence, vol. 3, pp. 1–24, November 2020.

[7] Guo J., Li Z., and Li M., "A Review on Prognostics Methods for Engineering Systems," IEEE Transactions on Reliability, vol. 69, no. 3, pp. 1110–1129, 2020.

[8] Ly C., Tom K., Byington C. S., Patrick R., and Vachtsevanos G. J., "Fault diagnosis and failure prognosis for engineering systems: A global perspective," 2009 IEEE International Conference on Automation Science and Engineering, CASE 2009, pp. 108–115, 2009.

[9] Cheng S., Azarian M. H., and Pecht M. G., "Sensor systems for prognostics and health management," Sensors, vol. 10, no. 6, pp. 5774–5797, 2010

[10] Daigle M. J. and Goebel K., "A model-based prognostics approach applied to pneumatic valves," International Journal of Prognostics and Health Management, vol. 2, no. 2, 2011.

[11] Fan J., Yung K. C., and Pecht M., "Physics-of-failure-based prognostics and health management for high-power white light-emitting diode lighting," IEEE Transactions on Device and Materials Reliability, vol. 11, no. 3, pp. 407–416, 2011.

[12] Vachtsevanos G. J., Lewis F. L., Roemer M. J., Hess A. J., and Wu B., "Intelligent fault diagnosis and prognosis for engineering systems," 2006, ch. 6, pp. 284–354, John Wiley and Sons, Ltd, 10.1002/9780470117842.ch6

[13] Gouriveau R., Medjaher K., and Zerhouni N., From Prognostics and Health Systems Management to Predictive Maintenance 1: Monitoring and Prognostics, vol 4, pp 1-163, 10 2016.

[14] Tian J., Morillo C., Azarian M. H., and Pecht M., "Kurtosis-Based Feature Extraction Coupled with K-Nearest Neighbor Distance Analysis," IEEE Trans. Ind. Electron., vol. 63, no. 3, pp. 1793–1803, 2016.

[15] Pecht M., "Chapter 150 Prognostics and Health Management," PRism, pp. 1–13, 1991.

[16] Zupan B., Demˇsar J., Kattan M. W., Beck J. R., and Bratko I., "Machine learning for survival analysis: A case study on recurrence of prostate cancer," Lecture Notes in Computer Science (including subseries Lecture Notes in Artificial Intelligence and Lecture Notes in Bioinformatics), vol. 1620, pp. 346–355, 1999.

[17] Xie C., Yang D., Huang Y., and Sun D., "Feature extraction and ensemble decision tree classifier in plant failure detection," Proceedings of the Annual Conference of the Prognostics and Health Management Society, PHM, pp. 727–735, 2015.

[18] Ibrahim N. A. and Kudus A., "Decision tree for prognostic classification of multivariate survival data and competing risks," in Recent Advances in Technologies, M. A. Strangio, Ed. Rijeka: IntechOpen, 2009, ch. 1., 10.5772/7429

[19] Jan S. U. and Koo I. S., "Sensor faults detection and classification using SVM with diverse features," in International Conference on Information and Communication Technology Convergence: ICT Convergence Technologies Leading the Fourth Industrial Revolution, ICTC 2017, vol. 2017-December. IEEE, pp. 576–578, oct 2017.

[20] Huang H. Z., Wang H. K., Li Y. F., Zhang L., and Liu Z., "Support vector machine based estimation of remaining useful life: current research status and future trends," Journal of Mechanical Science and Technology, vol. 29, no. 1, pp. 151–163, 2015.

[21] Loutas T. H., Roulias D., and Georgoulas G., "Remaining useful life estimation in rolling bearings utilizing data-driven probabilistic Esupport vectors regression," IEEE Transactions on Reliability, vol. 62, no. 4, pp. 821–832, 2013.

[22] Liu Z., Zuo M. J., and Qin Y., "Remaining useful life prediction of rolling element bearings based on health state assessment," Proceedings of the Institution of Mechanical Engineers, Part C: Journal of Mechanical Engineering Science, vol. 230, no. 2, pp. 314–330, 2016.

[23] Sun F., Li X., Liao H., and Zhang X., "A Bayesian least-squares support vector machine method for predicting the remaining useful life of a microwave component," Advances in Mechanical Engineering, vol. 9, no. 1, 2017.

ISBN: 978-0-9984188-3-4; Published online www.heatexchanger-fouling.com

[24] Tipping M. E., “Sparse Bayesian Learning and the Relevance Vector Machine,” Journal of Machine Learning Research, vol. 1, no. 3, pp. 211–244, 2001.
[25] Widodo A. and Yang B. S., “Application of relevance vector machine and survival probability to machine degradation assessment,” Expert Systems with Applications, vol. 38, no. 3, pp. 2592–2599, 2011, doi.org/10.1016/j.eswa.2010.08.049
[26] Hoang D. T. and Kang H. J., “Rolling element bearing fault diagnosis using convolutional neural network and vibration image,” Cognitive Systems Research, vol. 53, pp. 42–50, doi.org/10.1016/j.cogsys.2018.03.002, ,2019.
[27] Chao M. A., Kulkarni C., Goebel K., and Fink O., “Hybrid deep fault detection and isolation: Combining deep neural networks and system performance models,” no. Cm, pp. 1–25, 2019.
[28] Zhao R., Yan R., Chen Z., Mao K., Wang P., and Gao R. X., “Deep learning and its applications to machine health monitoring,” Mechanical Systems and Signal Processing, vol. 115, pp. 213–237, 2019.
[29] Kumar S., Torres M., Chan Y. C., and Pecht M., “A hybrid prognostics methodology for electronic products,” Proceedings of the International Joint Conference on Neural Networks, pp. 3479–3485, 2008.
[30] Sankavaram C., Pattipati B., Kodali A., Pattipati K., Azam M., Kumar S., and Pecht M., “Model-based and data-driven prognosis of automotive and electronic systems,” 2009 IEEE International Conference on Automation Science and Engineering, CASE 2009, pp. 96–101, 2009.
[31] Hale W. T., Safikou E., and Bollas G. M., “Inference of faults through symbolic regression of system data,” Computers and Chemical Engineering, vol. 157, p. 107619, 2022.
[32] Cheng S. and Pecht M., “Prediction of Electronic Products,” pp. 102– 107, 2009.
[33] Safikou Efi and Bollas George M., Fault detection and isolation in uncertain dynamic systems using composite optimization and inferential sensing, Computers & Chemical Engineering, Vol. 181,108509, ISSN 0098-1354, 2024.
[34] Yan M., Xie L., Muhammad I., Yang X., and Liu Y., “An effective method for remaining useful life estimation of bearings with elbow point detection and adaptive regression models,” ISA Transactions, vol. 128, pp. 290–300, 2021.
[35] Anis M. D., “Towards Remaining Useful Life Prediction in Rotating Machine Fault Prognosis: An Exponential Degradation Model,” 2018 Condition Monitoring and Diagnosis, CMD 2018 - Proceedings, 2018.
[36] Palmer K. A., Hale W. T., Such K. D., Shea B. R., and Bollas G. M., “Optimal design of tests for heat exchanger fouling identification,” Applied Thermal Engineering, vol. 95, pp. 382–393, feb 2016.

ISBN: 978-0-9984188-3-4; Published online www.heatexchanger-fouling.com